

## Breakdown of Traditional Many-Body Theories for Correlated Electrons

O. Gunnarsson,<sup>1</sup> G. Rohringer,<sup>2</sup> T. Schäfer,<sup>3</sup> G. Sangiovanni,<sup>4</sup> and A. Toschi<sup>3</sup>

<sup>1</sup>Max-Planck-Institut für Festkörperforschung, Heisenbergstraße 1, D-70569 Stuttgart, Germany

<sup>2</sup>Russian Quantum Center, Novaya street, 100, Skolkovo, Moscow region 143025, Russia

<sup>3</sup>Institute of solid state physics, Technische Universität Wien, 1040 Vienna, Austria

<sup>4</sup>Institute of Physics and Astrophysics, University of Würzburg, Würzburg 97074, Germany

(Received 31 March 2017; published 4 August 2017)

Starting from the (Hubbard) model of an atom, we demonstrate that the uniqueness of the mapping from the interacting to the noninteracting Green function,  $G \rightarrow G_0$ , is strongly violated, by providing numerous explicit examples of different  $G_0$  leading to the same physical  $G$ . We argue that there are indeed *infinitely* many such  $G_0$ , with numerous crossings with the physical solution. We show that this rich functional structure is directly related to the divergence of certain classes of (irreducible vertex) diagrams, with important consequences for traditional many-body physics based on diagrammatic expansions. Physically, we ascribe the onset of these highly nonperturbative manifestations to the progressive suppression of the charge susceptibility induced by the formation of local magnetic moments and/or resonating valence bond (RVB) states in strongly correlated electron systems.

DOI: 10.1103/PhysRevLett.119.056402

*Introduction.*—For more than 50 years, nonrelativistic quantum many-body theory (QMBT) has been successfully applied to describe the physics of many-electron systems in the field of condensed matter. Despite the intrinsic difficulty of identifying a small expansion parameter (analogously to the fine-structure constant of quantum electrodynamics), the formalism of QMBT—in its complementary representations in terms of Feynman diagrammatics [1,2] and of the universal Luttinger-Ward (LW) functional [3,4]—is the cornerstone of the microscopic derivation of Landau’s Fermi-liquid theory and of uncountable approximation schemes [5–9].

Yet, the actual conditions of applicability of the QMBT in the nonperturbative regime have been scarcely investigated. This is surprising because QMBT is extensively applied to strongly correlated electron materials, where band-theory and Fermi-liquid predictions fail, and some of the most exotic physics of condensed matter systems is observed. Recently, however, the quest for such investigations became particularly strong. This is because several cutting-edge QMBT approaches, explicitly designed for describing the crucial, but elusive, regime of intermediate-to-strong interactions, have been developed, e.g., the diagrammatic quantum Monte Carlo schemes [10] and numerous diagrammatic extensions [11–16] of dynamical mean-field theory (DMFT) [9,17].

Pioneering analyses of the perturbation theory breakdown have been reported in the past four years [18–27]. The main outcome can be summarized in two independent observations: (i) the occurrence of *infinitely* many singularities in the Bethe-Salpeter equations and (ii) the intrinsic multivaluedness of the LW functionals. The first problem appears as an infinite series of unexpected *divergences* in irreducible vertex functions [19], while the second is reflected in the

convergence of the perturbative series to an unphysical solution [20]. The intrinsic origin of these nonperturbative manifestations and their impact on the many-electron physics as well as on the method development in the field represent a challenge for the current theoretical understanding.

In this Letter, we report a fundamental progress in the comprehension of the perturbation theory breakdown and of its significance. In particular, going beyond the pioneering work of Ref. [20], (i) we show that there are many (probably an infinite number of) unphysical self-energies that become equal to the physical one at specific values of the interaction. This puts us into the position to (ii) demonstrate the actual correspondence between the vertex divergences of the Feynman diagrammatics and the occurrence of multiple branches of the LW functional. Finally, (iii) we generalize these results from the Hubbard atom to generic systems with strong correlations. Regarding the nature of the singularities, we show that vertex divergences of different kinds are reflected in different natures of the crossings of the branches.

The emerging scenario, which mathematically depicts an unexpectedly complex structure of the many-body formalism, will be physically related to the progressive suppression of charge fluctuations, a generic property of strongly correlated systems with a local interaction. The improved understanding of QMBT beyond the perturbative regime can serve as a guide for future developments of nonrelativistic many-electron algorithms.

*Multivaluedness of the Luttinger-Ward functional.*—The Luttinger-Ward functional  $\Phi[G]$  plays a crucial role in traditional many-body physics [4]. It is a universal functional of the full single-particle Green function  $G$ , which only depends on the interaction but not on the external potential. From  $\Phi[G]$  the free energy can be

determined. One can also obtain the electron self-energy  $\Sigma[G] \sim \delta\Phi[G]/\delta G$ , entering the Dyson equation,

$$G_0^{-1} - G^{-1} = \Sigma, \quad (1)$$

where  $G_0$  is the noninteracting Green function determined by the external potential. From  $\Sigma[G]$  one can compute all irreducible vertices  $\Gamma$  entering the Bethe-Salpeter equations [8] for response functions. For instance, the charge susceptibility is determined by the vertex [3,8,19,20]

$$\Gamma_c = \frac{\delta\Sigma[G]}{\delta G}. \quad (2)$$

Approximations built within this approach are guaranteed to be conserving [3]; therefore, it is exploited for numerous formal derivations [9,28–30]. Moreover, the full two-particle nature of the vertices  $\Gamma$  represents an ideal building block for approximations designed to preserve the Pauli principle properties and related sum rules. In this respect, it is believed that the parquet equations [8] are one of the most fundamental ways of performing diagrammatic summations.

In order for QMBT methods to be meaningful, an important property of the functional  $G[G_0]$  needs to be fulfilled: The introduction of  $\Sigma$  in QMBT implicitly assumes that there is a unique mapping between  $G$  and  $G_0$ ,  $G \rightarrow G_0$ . Otherwise, several branches of  $\Sigma$  would exist, corresponding to different  $G_0$ , posing the general problem of an intrinsic multivaluedness of any QMBT-based scheme. While—on the basis of general representability arguments [31,32]—only one of the possible branches of  $G_0$  can correspond to a noninteracting physical Hamiltonian, the existence of multiple  $G_0$  is not merely a formal issue. In fact, if two such branches cross,  $\Gamma$  in Eq. (2) might become ill defined and diverge. This would challenge important aspects of the traditional many-body theory, such as, e.g., the definition of physically meaningful parquet summations [33].

Figure 1 schematically illustrates such a scenario. The general functional relation between  $G$  and  $G_0$  is depicted by several red curves for different values of the electronic interaction  $U$  [34].  $G$  and  $G_0$  are here treated as numbers rather than functions (of frequency, momentum, spin, etc.). For  $U = 0$ ,  $G[G_0] = G_0$ , and for any physical  $G$  (horizontal blue line), the corresponding  $G_0$  is *univocally* determined. When  $U > 0$ , however,  $G[G_0]$  becomes “wavier,” displaying several maxima and minima in the functional space. This way, the intersection with  $G_{\text{phys}}$  would correspond to several  $G_0$  (blue dots), of which only one describes the physical system ( $G_0^{\text{phys}}$ ). Even if unphysical  $G_0$ ’s exist, many standard numerical algorithms are able to converge to the solution that is adiabatically connected with the  $U = 0$  one. This can, however, turn into an actual problem, *if* for some values of  $U$  the intersection with  $G_{\text{phys}}$  occurs at one extreme of  $G[G_0]$ . This would correspond to the intersection of two different solutions of  $G_0$  (and thus of  $\Sigma$ ; see green dashed lines in Fig. 1). At this point we would expect  $\delta G/\delta G_0 = 0$ .

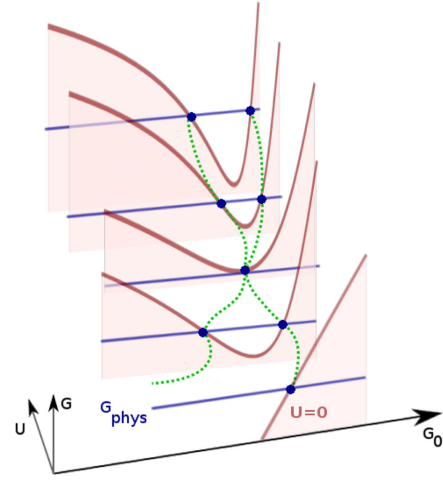


FIG. 1. Sketch of the functional  $G[G_0, U]$ , where  $G_0$  and  $G$  are assumed to be just numbers. The red curves correspond to cuts for different values of  $U$ , the horizontal blue lines show the corresponding values of  $G_{\text{phys}}$ , while the blue dots represent the  $G_0$  which produce  $G_{\text{phys}}$ .

Combining this with the Dyson equation and the definition [Eq. (2)] of  $\Gamma_c$ , one would conclude that  $\Gamma_c$  diverges.

To go beyond the sketch of Fig. 1, we present calculations for the Hubbard model [35] with one site (Hubbard atom) and show that different  $G_0$  indeed do cross for certain values of  $U$ . In Sec. I A of the Supplemental Material [36] we then show that such a crossing indeed does lead to divergences of  $\Gamma_c$ .

*Method.*—We have developed a method for finding different  $G_0$ ’s which lead to the physical  $G$  for the Hubbard atom. We use the Hirsch-Fye algorithm [40] to obtain  $G$  from a guess for  $G_0$ . This method involves a summation over auxiliary spins, which is usually done stochastically. Here we perform a complete summation using the Gray code [41], thereby avoiding stochastic errors. We guess a  $G_0$ , and then use a Metropolis method to search for improved guesses for  $G_0$ . When a promising guess has been found, the Hirsch-Fye equations are repeatedly linearized and solved, until a  $G_0$  has been found which accurately reproduces the physical  $G$  (see Sec. III of Ref. [36]). It is crucial that there are no stochastic errors in this approach. The method makes it possible to determine if two  $G_0$  really become equal for some  $U$  and to determine how they approach each other as  $U$  is varied.

*Results for the Hubbard atom.*—We start to present our results by showing in Fig. 2 (left)  $\text{Tr}\Sigma G_{\text{phys}}/(\beta U)$  as a function of  $U$  corresponding to the different  $G_0$  and, hence  $\Sigma$ , via Eq. (1). For  $G_0 = G_0^{\text{phys}} = 1/i\nu$ , this quantity yields the double occupancy (black curve). The colored (red and orange) curves are the results for the other (unphysical)  $G_0$ , collapsing to  $G_0^{\text{phys}}$  in the several crossing points shown in the figure. The latter ones *do* coincide—within our numerical accuracy—with the locations (marked by

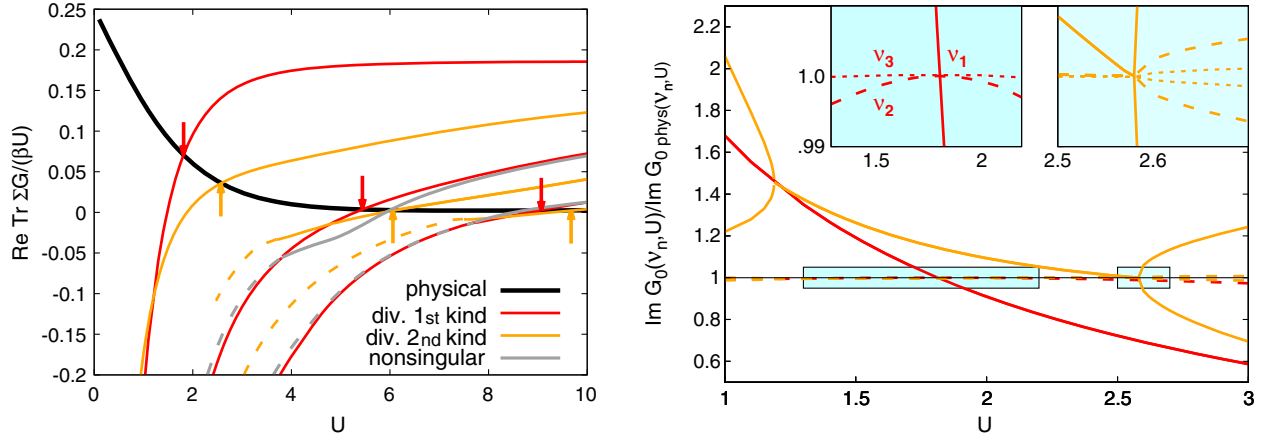


FIG. 2. Left:  $\text{Tr} \Sigma G / (\beta U)$  as a function of  $U$  corresponding to different  $G_0$  for the Hubbard atom for  $\beta = 2$ . Red and orange arrows mark the divergences of  $\Gamma_c$  according to Ref. [19]. The curve corresponding to  $G_0^{\text{phys}}$  is shown in black. Beyond the red and orange curves, one finds further crossings (gray lines) for which, however,  $G_0(\nu) \neq G_0^{\text{phys}}(\nu)$  and, hence, no divergence of  $\Gamma_c$  is found (see Sec. IC of the Supplemental Material [36]). Dashed curves indicate that  $\text{Tr} \Sigma G / (\beta U)$  also has an imaginary contribution (not shown). Right: Imaginary part of  $G_0$  (normalized to  $\text{Im} G_0^{\text{phys}}$ ) for the first red and orange curves. Results for the lowest (bold lines), second lowest (dashed lines), and (in insets) third lowest (dotted lines)  $|\nu_n|$  are shown.

vertical arrows) of the first six divergences of  $\Gamma_c$  in the Hubbard atom [19]. The red  $G_0$ 's are associated with a milder violation of physical constraints than the orange ones [e.g., the former can acquire a nonzero real part, but the latter can even violate the generic condition:  $G_0(\nu) = G_0(-\nu)^*$  [36]]. The left-hand red curve was found by Kozik *et al.* [20], although, there, it could not be converged around the crossing with  $G_0^{\text{phys}}$ .

There are important connections between the frequency dependence of the divergences of  $\Gamma_c$ , coded by red and orange colors [19], and the detailed behavior of  $G_0$  at a crossing. The divergences of  $\Gamma_c$  can be divided into two classes [18,19]. To this end, we consider the generalized charge susceptibility  $\chi_c^{\nu\nu'(\omega=0)}$  [42], which depends on two fermionic Matsubara frequencies,  $\nu$  and  $\nu'$ , and a bosonic frequency  $\omega = 0$ .  $\Gamma_c$  is then given by

$$\Gamma_c = \beta^2 [\chi_c^{-1} - \chi_0^{-1}], \quad (3)$$

where  $\chi_0$  is the noninteracting generalized susceptibility and  $\chi_c$  and  $\chi_0$  are treated as matrices of  $\nu$  and  $\nu'$ . These matrices can be diagonalized,

$$\chi_c^{\nu\nu'(\omega=0)} = \sum_l V_l(\nu)^* \varepsilon_l V_l(\nu'), \quad (4)$$

with  $V_l(\nu)$  and  $\varepsilon_l$  being the corresponding eigenvectors and eigenvalues. While the divergences of  $\Gamma_c$  always correspond to the vanishing of one  $\varepsilon_l$ , they differ in the frequency structure of  $V_l(\nu)$ : For the divergences marked by the red arrows,  $V_l(\nu)$  has only two nonzero elements [at  $\nu = \pm\nu_n = \pm(2n-1)\pi/\beta$ , with  $n = 1, 2, \dots$ ], reflecting a *localized* divergence at  $\nu = \pm\nu_n$ , while for the orange arrows,  $V_l(\nu) \neq 0 \forall \nu$ , reflecting a *global* divergence of  $\Gamma_c$  [19].

An analogous classification is also applicable to the different  $G_0$  resolved in frequency space: In Fig. 2 (right) we plot the ratio  $\text{Im} G_0(\nu) / \text{Im} G_0^{\text{phys}}(\nu)$  corresponding to the first two crossings for the three lowest  $\nu$ . As  $G_0^{\text{phys}}$  is purely imaginary, the condition  $G_0(\nu) = G_0^{\text{phys}}(\nu)$  is reflected in their ratio being 1 and  $\text{Re} G_0 / \text{Im} G_0^{\text{phys}} = 0$  (shown in Supplemental Material [36]). Figure 2 (right) demonstrates that the red and orange crossings observed in  $\text{Tr} \Sigma G_{\text{phys}}$  indeed correspond to an actual identity of  $G_0(\nu) = G_0^{\text{phys}}(\nu) \forall \nu$ , both at  $U = 1.81$  (red) and  $2.58$  (orange). Yet, the corresponding zooms in the insets show a *qualitative* difference between the two cases. For the red case, the crossing of  $G_0$  with  $G_0^{\text{phys}}$  is *linear* in  $U$  only for  $\nu = \pi/\beta$  (solid line), while it is  $O(U^2)$  for all other  $\nu_n$  (dashed line). In the orange case, the crossings display the *same* behavior for all the frequencies; see insets of Fig. 2 and the discussion in Sec. IA of Ref. [36]. There, an analytical proof is given that this leads to a divergence of  $\Gamma_c$  for  $\nu, \nu' = \pm\pi/\beta$  at the red crossing and for all frequencies at the orange crossing. Similar results are found for the second and third red and orange crossings, but for the former the linear crossing happens for  $\nu_2 = 3\pi/\beta$  (second) and  $\nu_3 = 5\pi/\beta$  (third). This is consistent with the result in Ref. [19] that the corresponding divergences of  $\Gamma_c$  happen at these specific  $\nu_n$ .

The one-to-one correspondence of red (orange) crossings with the local (global) divergences of  $\Gamma_c$  illustrates how the heuristic scenario of Fig. 1 is actually realized for the Hubbard atom. The result also indicates the existence of an *infinite* number of unphysical  $G_0$ , since *infinitely* many red and orange divergences were found for the Hubbard atom [19]. Furthermore, there are indications that the infinity of the total number of  $G_0$  might be of a higher cardinality than

that of the vertex divergences, as we discuss in Sec. IV of Ref. [36].

*Generic strongly correlated systems.*—To make closer contact to strongly correlated physical systems, we consider the Hubbard model in DMFT [9,17], where the Hubbard atom is embedded in a self-consistent, noninteracting host. The LW functional is unchanged, since it only depends on the interacting part of the Hamiltonian. The external-potential part, however, changes, and therefore both  $G_{\text{phys}}$  and  $G_0^{\text{phys}}$  are different. We can exploit the relation of the crossings with the divergences of  $\Gamma_c$  and the zero eigenvalues in Eq. (4), and gain further insight by analyzing the physical local charge susceptibility. In DMFT, this is given by [33]

$$\chi_{\text{ch}} = \frac{1}{\beta^2} \sum_{\nu\nu'} \chi_c^{\nu\nu'}(\omega=0) = \frac{1}{\beta^2} \sum_l \varepsilon_l \left| \sum_{\nu} V_l(\nu) \right|^2. \quad (5)$$

The corresponding DMFT results are reported in Fig. 3. By increasing  $U$ , the electrons gradually localize, building up local magnetic moments with longer lifetimes. These, in turn, freeze the local charge dynamics, with  $\chi_{\text{ch}}$  becoming very small especially in the proximity of or after the Mott metal-insulator transition (in the range  $U = 2.3$ – $2.4$  for  $\beta = 40$ ). While the physics of this generic trend is known, the projection of  $\chi_{\text{ch}}$  in its eigenvalue basis yields highly nontrivial information. We analyze  $\chi_{\text{ch}}$  in terms of the contributions from positive and negative  $\varepsilon_l$ . For small and moderate  $U$ , all  $\varepsilon_l$  are positive. As  $U$  increases, one  $\varepsilon_l$  after the other goes through zero (see inset of Fig. 3). Each time  $\Gamma_c$  diverges [see Eqs. (3) and (4)], a new  $G_0$  becomes identical to  $G_0^{\text{phys}}$ , and the negative component of  $\chi_{\text{ch}}$  becomes more important. Such a negative component of  $\chi_{\text{ch}}$  plays a crucial role in realizing the correct strong-coupling physics. Neglecting it would lead to a  $\chi_{\text{ch}}$

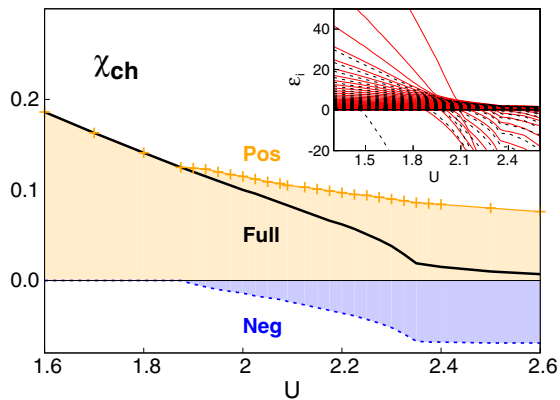


FIG. 3. DMFT calculation of the local charge susceptibility ( $\chi_{\text{ch}}$ ) [Eq. (5)] (black line) as a function of  $U$  for a two-dimensional Hubbard model at half filling, with half bandwidth  $4t = 1$  at  $\beta = 40$ . Both  $\chi_{\text{ch}}$  and its contributions from positive (orange) and negative (blue) eigenvalues ( $\varepsilon_l$ ) are shown. The inset shows the  $U$  dependence of  $\varepsilon_l$  [solid (dashed) lines for  $\varepsilon_l$  with  $V_l(\nu) = (-1)V_l(-\nu)$ ].

approximately saturating at some sizable value in the Mott phase, instead of being strongly suppressed. We also note that a small value of  $\chi_{\text{ch}}$  in itself is not sufficient for this scenario to be realized (e.g., in a dilute system  $\chi_{\text{ch}}$  can be small, but all  $\varepsilon_l > 0$ ). Here, the crucial factor is the mechanism responsible for the reduction of  $\chi_{\text{ch}}$ : the gradual local moment formation which manifests itself in a progressively larger contribution of the negative  $\varepsilon_l$ . This is, thus, the underlying physics responsible for the occurrence of the (infinitely many) unphysical  $G_0$  crossing  $G_0^{\text{phys}}$ , and the related divergences of  $\Gamma_c$ . This also applies to the corresponding breakdown of perturbative expansions, such as parquet-based approximations. A certain class of diagrams can give a positive infinite contribution, which is canceled by another class of diagrams [33]. Then the diagrammatic expansion is not absolutely convergent, as was also found in Ref. [20]. This makes conventional diagrammatic expansions highly questionable for intermediate-to-strong correlations. While it is not surprising that perturbative approaches might break down at the Mott transition, it is interesting that this happens well before the Mott transition occurs, where Fermi-liquid physical properties still control the low-energy physics.

It is important to stress that the nonperturbative manifestations discussed in this Letter are affecting not *only* models dominated by purely local physics (such as the Hubbard atom or its DMFT version). In fact, divergences of  $\Gamma_c$  have also been found [33] studying the two-dimensional Hubbard model, by means of the dynamical cluster approximation [29]. In this case, the underlying physics behind the change of sign of the  $\varepsilon_l$  could be related to the formation of a RVB state [43], also responsible [44] for the opening of a spectral pseudogap [45]. Increasing the size of the cluster in the dynamical cluster approximation might even push the occurrence of the first  $\varepsilon_l = 0$  and the pseudogap towards lower  $U$ , due to strong antiferromagnetic fluctuation extended on larger length scales [33,46,47].

*Conclusions.*—We have reported important progress towards the understanding of the mathematical structures of quantum many-body theories in the nonperturbative regime, and of the physics behind them. The structure of the LW functionals is even richer than the pioneering work by Kozik *et al.* suggested [20]: We find a very large, probably *infinite*, number of noninteracting  $G_0$  leading to the same dressed  $G$ . This can be regarded as a formal problem, to be treated by means of a restriction to the domain of the physical  $G_0$ 's [27,31,32], as long as the unphysical and physical  $G_0$  do not intersect. However, in the nonperturbative regime we find many crossings. These crossings reflect the analytical structure of the LW functional for interacting systems. We show that they lead to divergences of irreducible vertex functions. This challenges current quantum many-body algorithms in several respects, e.g., causing noninvertibility of the Bethe-Salpeter equation and breakdown of the parquet resummations. These

problems, which occur when the correlation is still substantially weaker than in a Mott insulator, originate, nonetheless, in underlying strong-coupling physical mechanisms, which also control the formation of local moments and RVB states. This is reflected in the progressive suppression of the charge susceptibility in correlated systems. Further investigations of the theoretical foundations beyond the perturbative regime should play a central role for future method developments in condensed matter physics.

We thank S. Ciuchi, P. Chalupa, P. Thunström, M. Capone, S. Andergassen, and K. Held for insightful discussions. The authors would like to thank all attendees to the Workshop “Multiple Solutions in Many-Body Theories” held in Paris for interesting discussions. A. T. also thanks the group of A. Rubtsov for the hospitality at the Russian Quantum Center. We acknowledge support from FWF through Project No. I 2794-N35 (T. S. and A. T.) and from the research unit FOR 1346 of the DFG (G. S.).

- 
- [1] A. A. Abrikosov, L. P. Gorkov, and F. A. Davis, *Methods of Quantum Field Theory in Statistical Physics* (Dover, New York, 1963).
- [2] A. L. Fetter and J. D. Valecka, *Quantum Theory of Many-Particle Systems* (McGraw-Hill, New York, 1971).
- [3] G. Baym and L. P. Kadanoff, *Phys. Rev.* **124**, 287 (1961).
- [4] J. M. Luttinger and J. C. Ward, *Phys. Rev.* **118**, 1417 (1960).
- [5] L. Hedin and S. Lundqvist, *Solid State Phys.* **23**, 1 (1970).
- [6] N. E. Bickers, D. J. Scalapino, and S. R. White, *Phys. Rev. Lett.* **62**, 961 (1989).
- [7] W. Metzner, M. Salmhofer, C. Honerkamp, V. Meden, and K. Schönhammer, *Rev. Mod. Phys.* **84**, 299 (2012).
- [8] For a review, see, e.g., N. E. Bickers, *Int. J. Mod. Phys. B* **05**, 253 (1991); *Theoretical Methods for Strongly Correlated Electrons*, edited by D. Senechal, A. Tremblay, and C. Bourbonnais (Springer-Verlag, New York, 2004), Chap. 6.
- [9] A. Georges, G. Kotliar, W. Krauth, and M. Rozenberg, *Rev. Mod. Phys.* **68**, 13 (1996).
- [10] K. Van Houcke, E. Kozik, N. Prokof'ev, and B. Svistunov, in *Computer Simulation Studies in Condensed Matter Physics XXI*, edited by D. Landau, S. Lewis, and H. Schuttler (Springer-Verlag, Berlin, 2008); E. Kozik, K. V. Houcke, E. Gull, L. Pollet, N. Prokof'ev, B. Svistunov, and M. Troyer, *Europhys. Lett.* **90**, 10004 (2010).
- [11] A. Toschi, A. A. Katanin, and K. Held, *Phys. Rev. B* **75**, 045118 (2007).
- [12] A. N. Rubtsov, M. I. Katsnelson, and A. I. Lichtenstein, *Phys. Rev. B* **77**, 033101 (2008).
- [13] A. N. Rubtsov, M. I. Katsnelson, and A. I. Lichtenstein, *Ann. Phys. (Amsterdam)* **327**, 1320 (2012).
- [14] G. Rohringer, A. Toschi, H. Hafermann, K. Held, V. I. Anisimov, and A. A. Katanin, *Phys. Rev. B* **88**, 115112 (2013).
- [15] T. Ayral and O. Parcollet, *Phys. Rev. B* **92**, 115109 (2015); **93**, 235124 (2016).
- [16] T. Ayral and O. Parcollet, *Phys. Rev. B* **94**, 075159 (2016).
- [17] W. Metzner and D. Vollhardt, *Phys. Rev. Lett.* **62**, 324 (1989); M. Jarrell, *Phys. Rev. Lett.* **69**, 168 (1992).
- [18] T. Schäfer, G. Rohringer, O. Gunnarsson, S. Ciuchi, G. Sangiovanni, and A. Toschi, *Phys. Rev. Lett.* **110**, 246405 (2013).
- [19] T. Schäfer, S. Ciuchi, M. Wallerberger, P. Thunström, O. Gunnarsson, G. Sangiovanni, G. Rohringer, and A. Toschi, *Phys. Rev. B* **94**, 235108 (2016).
- [20] E. Kozik, M. Ferrero, and A. Georges, *Phys. Rev. Lett.* **114**, 156402 (2015).
- [21] V. Janiš and V. Pokorný, *Phys. Rev. B* **90**, 045143 (2014).
- [22] T. Ribic, G. Rohringer, and K. Held, *Phys. Rev. B* **93**, 195105 (2016).
- [23] A. Stan, P. Romaniello, S. Rigamonti, L. Reining, and J. A. Berger, *New J. Phys.* **17**, 093045 (2015).
- [24] R. Rossi and F. Werner, *J. Phys. A* **48**, 485202 (2015).
- [25] G. Lani, P. Romaniello, and L. Reining, *New J. Phys.* **14**, 013056 (2012).
- [26] R. Rossi, F. Werner, N. Prokof'ev, and B. Svistunov, *Phys. Rev. B* **93**, 161102(R) (2016).
- [27] W. Tarantino, P. Romaniello, J. A. Berger, and L. Reining, *Phys. Rev. B* **96**, 045124 (2017).
- [28] J. M. Luttinger, *Phys. Rev.* **119**, 1153 (1960).
- [29] T. Maier, M. Jarrell, T. Pruschke, and M. H. Hettler, *Rev. Mod. Phys.* **77**, 1027 (2005).
- [30] L. Pollet, N. V. Prokof'ev, and B. V. Svistunov, *Phys. Rev. B* **83**, 161103 (2011); S. Biermann, F. Aryasetiawan, and A. Georges, *Phys. Rev. Lett.* **90**, 086402 (2003).
- [31] M. Potthoff, *Eur. Phys. J. B* **32**, 429 (2003).
- [32] M. Potthoff, *Condens. Matter Phys.* **9**, 557 (2006).
- [33] O. Gunnarsson, T. Schäfer, J. P. F. LeBlanc, J. Merino, G. Sangiovanni, G. Rohringer, and A. Toschi, *Phys. Rev. B* **93**, 245102 (2016).
- [34] Actually, this representation corresponds to the so-called one-point model; see, e.g., Refs. [23–26].
- [35] J. Hubbard, *Proc. R. Soc. A* **276**, 238 (1963); M. C. Gutzwiller, *Phys. Rev. Lett.* **10**, 159 (1963); J. Kanamori, *Prog. Theor. Phys.* **30**, 275 (1963).
- [36] See Supplemental Material at <http://link.aps.org/supplemental/10.1103/PhysRevLett.119.056402> for further analytical derivations and numerical results, which also includes Refs. [37–39].
- [37] J. Hubbard, *Phys. Rev. Lett.* **3**, 77 (1959).
- [38] J. E. Hirsch, *Phys. Rev. B* **28**, 4059 (1983).
- [39] F. J. Dyson, *Phys. Rev.* **85**, 631 (1952).
- [40] J. E. Hirsch and R. M. Fye, *Phys. Rev. Lett.* **56**, 2521 (1986).
- [41] F. Gray, U.S. Patent No. 2632,058 (1953); C. D. Miller, *Binary Numbers and the Standard Gray Code. Mathematical Ideas*, 9th ed. (Addison-Wesley, Reading, MA, 2000), Chap. 4.
- [42] G. Rohringer, A. Valli, and A. Toschi, *Phys. Rev. B* **86**, 125114 (2012).
- [43] P. W. Anderson, *Science* **235**, 1196 (1987); S. Liang, B. Doucot, and P. W. Anderson, *Phys. Rev. Lett.* **61**, 365 (1988).
- [44] J. Merino and O. Gunnarsson, *J. Phys. Condens. Matter* **25**, 052201 (2013); *Phys. Rev. B* **89**, 245130 (2014).
- [45] T. Timusk and B. Statt, *Rep. Prog. Phys.* **62**, 61 (1999).
- [46] T. Schäfer, F. Geles, D. Rost, G. Rohringer, E. Arrigoni, K. Held, N. Blümer, M. Aichhorn, and A. Toschi, *Phys. Rev. B* **91**, 125109 (2015).
- [47] O. Gunnarsson, T. Schäfer, J. P. F. LeBlanc, E. Gull, J. Merino, G. Sangiovanni, G. Rohringer, and A. Toschi, *Phys. Rev. Lett.* **114**, 236402 (2015).